# Distribution patterns of long-runout landslides triggered by the Northern Nagano Prefecture Earthquake of 2011

Takashi KIMURA[1,*], Kazuhiro HATADA[2], Shin'ya KATSURA[1],
Kiyoteru MARUYAMA[1], Kazuya AKIYAMA[1], and Tomoyuki NORO[3]
[1] Snow avalanche and Landslide Research Center, Public Works Research Institute, Japan
[2] Nippon Koei Co., Ltd., Japan
[3] Research Faculty of Agriculture, Hokkaido University, Japan
*Corresponding author. E-mail: t-kimura55@pwri.go.jp

## INTRODUCTION

The northern Nagano Prefecture earthquake of 12 March 2011 caused many long-runout landslides. Although the major reason for the long runout is considered to be the abundant snow at the time of the earthquake, other factors that influenced the occurrence and spatial distribution of long-runout landslides remained unknown. To clarify the primary causes and distribution patterns of long-runout landslides, this study conducted detailed interpretations of aerial photographs and GIS analyses.

## STUDY SITE

A series of high-resolution aerial photographs (14 cm per pixel of ground resolution) covering about 200 $km^2$ of northern Nagano Prefecture and southern Niigata Prefecture was taken on the day of the earthquake. In this area, a 73 $km^2$ study site was established in a mountainous region in the hanging wall of the seismogenic fault (Fig. 1). The study site was divided along the main ridge line of Higashi-kubiki Hill into Sakae-Tsunan area (ST; 50 $km^2$) and Tokamachi area (TK; 23 $km^2$). ST consists of Neogene to Quaternary volcanic rocks and sedimentary rocks, whereas TK consists mainly of Neogene sedimentary rocks. The distances to the fault were less than 6.5 km for ST and ranged from 4.2–8.8 km for TK. A 227-cm snow depth was recorded on 12 March 2011 (JMA Tsunan station: Fig. 1).

## METHODS

The high-resolution aerial photographs taken in the area of deep snow cover allowed us to identify the degree of disruption of the mass that occurred in the movement process. For each landslide, the landslide slope and transfer/deposition zone of the displaced mass including snow-mixed debris were delineated, then classified into two types of movement: slide type, in which the mass with its (partly disrupted) snow layer covered more than 50% of the area of the landslide slope, and failure type, in which the severely disrupted mass and snow layer covers less than 50% of the area of the landslide slope. Using a GIS software, the horizontal length of the landslide slope ($L1$), the travel distance of the mass ($L2$), areas of the landslide slope and the mass were measured for each landslide, and the traveling ratio ($Tr=L2/L1$) was calculated. Slope gradients within the study site and the mean gradient for each landslide slope were calculated based on 10-m DEMs. These data were summarized for each area.

## RESULTS

Eighty-two landslides were identified within the study site. Landslide numbers per unit area of the two areas were similar (ST: 1.14 slides/km$^2$, TK: 1.09 slides/km$^2$), but the percentage of area affected by landslides in ST (1.37%) was 2.5 times larger than that in TK (0.54%). The failure-type landslides were denser in ST (ST: 0.92 slides/km$^2$, TK: 0.65 slides/km$^2$), while the slide-type landslides had reverse proportion (ST: 0.22 slides/km$^2$, TK: 0.44 slides/km$^2$). These results indicate that ST is more prone to large-scale failure-type landslides. In both two areas, the slope gradient frequency peaked at 20° for hillslopes and at 30-45° for landslides (Fig. 2). Although about 60% of the failure-type landslides was consisted of small-size landslides with $L1$ <100 m, many of them traveled long distances over their slope lengths (Fig. 3). Moreover, the travel distance of the failure-type landslides showed a clear increase tendency as slope length become larger (Fig. 3).

## CONCLUSIONS

Despite similarity in the number of landslides per unit area and frequency distributions of the slope gradients of hillslopes and landslide slopes between the two areas, long-runout landslides were clearly concentrated in ST, reflecting slope susceptibility to large-scale failure. The results indicate that even within a narrow area in the hanging wall, the occurrence of long-runout landslides can vary depending on mass movement type and landslide size.

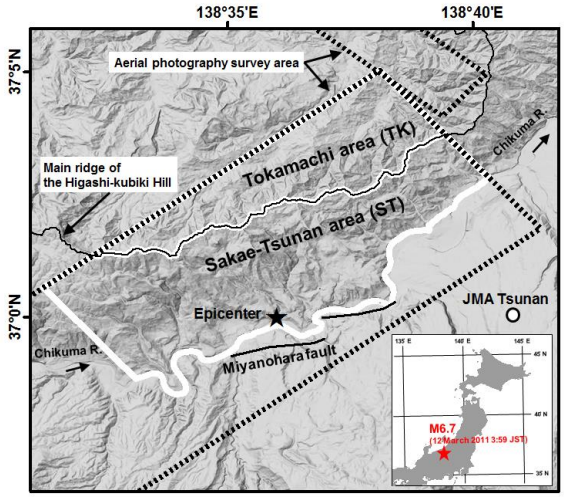


**Fig. 1** Location map of the study site

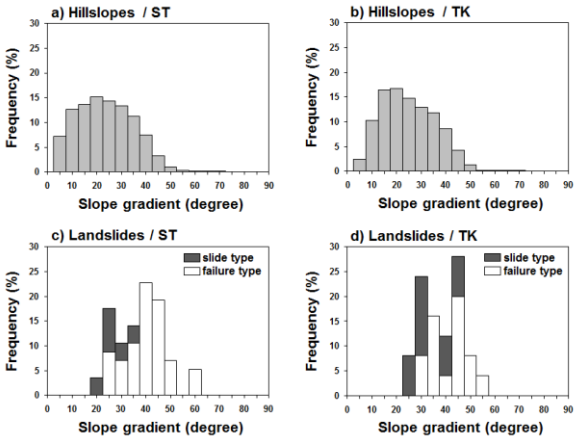


**Fig. 2** Frequency distributions of slope gradient

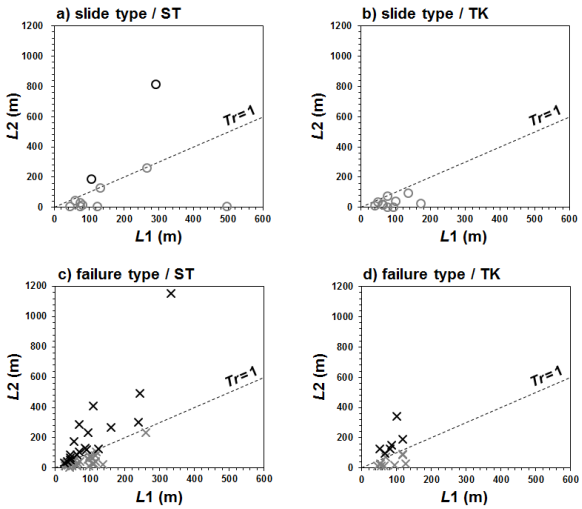


**Fig. 3** Relationships between $L1$ and $L2$ of the landslide

**Keywords: earthquake-triggered landslide, air photo interpretation, travel distance, landslide distribution, snowfall period**